

# Multi-Pass Receptors

James A. Wells, Editor



c00023

# Structure and Function of G-Protein-Coupled Receptors: Lessons from Recent Crystal Structures

Thomas P. Sakmar

Laboratory of Molecular Biology and Biochemistry, The Rockefeller University, New York, New York

## s0010 INTRODUCTION

p0010

The crystal structure of the rod cell visual pigment, rhodopsin, was reported in 2000, and allowed the critical evaluation of a decade of earlier structure–activity relationship (SAR) studies. Recent reports of crystal structures of additional G-protein-coupled receptors (GPCRs) and of a ligand-free opsin now provide an opportunity to compare and contrast modes of ligand binding and G-protein activation among the entire superfamily of heptahelical receptors. For example, crystal structures of engineered human  $\beta_2$  adrenergic receptors (ARs) in complex with an inverse agonist ligand, carazolol, provide three-dimensional snapshots of the disposition of its seven transmembrane helices and the ligand binding site. As expected,  $\beta_2$ AR shares substantial structural similarities with rhodopsin. However, although carazolol and the 11-*cis*-retinylidene chromophore of rhodopsin, which acts as an inverse agonist, are situated in the same general binding pocket, the second extracellular (E2) loop structures are quite distinct. E2 in rhodopsin shows  $\beta$ -sheet structure and forms part of the chromophore binding site. In the  $\beta_2$ AR, E2 is  $\alpha$ -helical and seems to be distinct from the receptor's active site, allowing a potential entry pathway for diffusible ligands. The structure of an engineered human A2A adenosine receptor in complex with the subtype specific antagonist ZM241385 provides a number of additional surprises. The ligand binds to the A2A adenosine receptor in an extended conformation essentially perpendicular to the plane of the membrane. Structures of ligand-free opsin and of opsin in complex with a peptide corresponding to the carboxyl-terminal tail of its cognate G-protein  $\alpha$  subunit, which probably represent the active-state structure of the receptor, strongly support the “helix movement model” of receptor activation. Compared with the

structure of rhodopsin, the opsin structures show prominent structural changes in the highly conserved E(D)RY and NpxxY(x)5,6F regions, and in transmembrane helices 5, 6 and 7 (H5–H7). Remarkably H6 is tilted outward by 6–7 Å in the opsin structure. These new structures, together with extensive SAR data from earlier studies, provide insight about structural determinants of ligand specificity, and suggest how the binding of agonist ligands might cause the structural changes that activate GPCRs.

## RECENT ADVANCES IN STRUCTURAL STUDIES OF G-PROTEIN-COUPLED RECEPTORS

s0020

GPCR signaling complexes are allosteric machines. Agonist receptor ligands outside of the cell induce guanine-nucleotide exchange on a heterotrimeric guanine-nucleotide binding regulatory protein (G protein) inside of the cell where the ligand binding site on the receptor and the nucleotide binding site and the G protein are in the order of 8–10 nm or more apart. Additional non-canonical signaling pathways facilitate cross-talk between linear GPCR-signaling pathways and receptor tyrosine kinase (RTK)-mediated signaling pathways. Receptor phosphorylation by receptor-specific kinases and the binding of various cellular adaptor proteins also regulates receptor desensitization, internalization, sequestration, and recycling. Receptor oligomerization, or in some cases hetero-oligomerization, is thought to modulate receptor cell-surface expression, ligand binding affinity, and downstream signaling specificity for at least some classes of GPCRs. Heptahelical receptors are also arguably the most important single class of pharmaceutical drug targets in the human genome. According to Overington *et al.* [1], of the

p0020

266 human targets for approved drugs, a remarkable 27 percent correspond to rhodopsin-like, or Family A, GPCRs. GPCRs will remain important drug targets in the foreseeable future, especially since well over 100 of the estimated 726 heptahelicals encoded by the human genome remain “orphan” receptors and most of these are expressed in the central nervous system. Orphan receptors are expressed but have no known exogenous ligand, although such ligands are presumed to exist.

monoaminergic turkey  $\beta_1$ AR [14], engineered expressed human A2A adenosine receptor [15], squid rhodopsin [16–17], and ligand-free opsins [18–19]. Table 23.1 shows the complete list of structures currently available.

**TABLE 23.1** GPCR crystal structures

Receptor structure	PDB Code	Resolution (Å)	Reference
Bovine rhodopsin	1F88	2.8	Palczewski <i>et al.</i> [7]
Bovine rhodopsin	1HZX	2.8	Teller <i>et al.</i> [37]
Bovine rhodopsin	1L9H	2.6	Okada <i>et al.</i> [38]
Bovine rhodopsin	1U19	2.2	Okada <i>et al.</i> [39]
Bovine rhodopsin	1GZM	2.65	Li <i>et al.</i> [40]
Bovine rhodopsin photoproduct	2I35-37	4.15	Salom <i>et al.</i> [41]
Bovine bathorhodopsin	2G87	2.6	Nakamichi and Okada [8]
Bovine lumirhodopsin	2HPY	2.8	Nakamichi and Okada [9]
Bovine isorhodopsin	2PED	2.95	Nakamichi <i>et al.</i> [10]
Expressed engineered bovine rhodopsin	2J4Y	3.4	Standfuss <i>et al.</i> [42]
Expressed engineered human $\beta_2$ adrenergic receptor	2RH1	2.4	Cherezov <i>et al.</i> [11]
Expressed engineered human $\beta_2$ adrenergic receptor	2R4R/S	3.4/3.7	Rasmussen <i>et al.</i> [13]
Squid rhodopsin	2Z73	2.5	Murakami and Kouyama [16]
Squid rhodopsin	2Z1Y	3.7	Shimamura <i>et al.</i> [17]
Expressed engineered human $\beta_2$ adrenergic receptor	3D4S	2.8	Hanson <i>et al.</i> [43]
Expressed engineered turkey $\beta_1$ adrenergic receptor	2VT4	2.7	Warne <i>et al.</i> [14]
Bovine opsin	3CAP	2.9	Park <i>et al.</i> [18]
Bovine opsin	3DQB	3.2	Scheerer <i>et al.</i> [19]
Expressed engineered human A2A adenosine receptor	3EML	2.6	Jaakola <i>et al.</i> [15]

t0010

p0030

The concepts of affinity and efficacy are used to describe the pharmacology of a drug (ligand). Affinity refers to the ability of the drug to bind to its molecular target, and efficacy refers to the ability of a drug to induce a biological response in its molecular target. Partial agonists exhibit less efficacy compared with (full) agonists. Neutral antagonists do not change the basal activity of the receptor (zero efficacy), and inverse agonists are able to stabilize the inactive state of the receptor. They essentially exhibit inversion of efficacy. Initially, in classical work, medicinal chemistry and pharmacology studies generated a vast inventory of SAR data. Receptor subtypes were defined by specific ligands (mostly antagonists) and validated in tissue physiology models, if available. With the cloning and heterologous expression of receptors (and chimeric/mutant receptors), a second generation of experiments led to mapping of ligand binding sites on receptors representing members of the main pharmacological targets (muscarinic,  $\alpha$  and  $\beta$  adrenergic, dopamine, and serotonin receptors). However, only relatively few subtypes were analyzed in this way. The third generation of experiments was focused on mutagenesis-based structure determination to map the interactions between the highly conserved residues on TM helices, which, together with the bacteriorhodopsin structure and the available three-dimensional low-resolution cryo-electron microscopy projection structures of rhodopsin, resulted in the first models of the TM domains of a larger series of homologous receptors. The fourth generation of experiments focused on the dynamics of receptor activation, culminating in the “helix movement model” of receptor activation and some level of understanding of the structural basis for constitutive receptor activity and constitutively-activating mutations (CAMs) [2–6]. Today, with a new generation of receptor structures, we are finally able to compare and contrast the high-resolution structure of rhodopsin with that of other GPCRs on the background of deduced primary structures of a substantial number of related receptors from various genomes.

p0040

In a landmark report in 2000, a high-resolution crystal structure for rhodopsin, from bovine rod cells, was reported [7]. In the past few years, additional structures of rhodopsin and of thermally trapped early photoproducts of rhodopsin with all-*trans*-retinylidene chromophore have also been reported [8–10]. Most recently, high-resolution crystal structures of a number of additional GPCRs have become available: engineered expressed monoaminergic human  $\beta_2$  adrenergic receptors (ARs) [11–13], engineered expressed

## CRYSTAL STRUCTURES OF HUMAN $\beta_2$ AR

The crystal structures of the  $\beta_2$ AR provide a excellent data set to carry out a detailed analysis of ligand binding principles in Family A GPCRs, as has been recently reviewed [20]. The crystal structure of an engineered human  $\beta_2$ AR consists of a receptor construct modified at the N-terminus by addition of a hemagglutinin (HA) signal sequence followed by a FLAG epitope [13]. The receptor was truncated after position 365 so that it lacks 48 amino acid residues at its C-terminus. A glycosylation site was also removed by site-directed mutagenesis (N187E). A second receptor construct was also crystallized that contained a Tobacco Etch Virus (TEV) protease cleavage site so that the receptor lacked 24 amino acids from the N-terminus after proteolysis. The receptor clones were expressed in *Sf9* insect cells, solubilized in dodecylmaltoside detergent, and purified by successive antibody affinity and ligand (alprenolol) affinity chromatography. N-linked glycosylation was removed by glycosidase treatment and the FLAG epitope was removed where possible with the AcTEV protease, an enhanced form of TEV protease. The purified protein was relatively stable, but only about one-half of the purified receptors appeared to be functional and capable of ligand binding.

A monoclonal antibody was developed in parallel that binds to the C3 loop of the native receptor, but not to denatured receptor protein. Fab fragments were prepared and reacted with the purified receptor, which was further stabilized by carazolol, an inverse agonist ligand with  $\mu$ M affinity. The resulting complex was purified by size-exclusion chromatography, and mixed with bicelles composed of the phospholipid DMPC and the detergent CHAPSO suitable for crystallization trials. Long, thin, plate-like crystals were cryoprotected, and an entire data set was collected from a single crystal. Although the initial resolution was about 3.0 Å, the diffraction was somewhat anisotropic and the resolution of the final model was 3.4 Å in the plane of the putative membrane, and 3.7 Å perpendicular to the plane of the membrane. The final structures (one for each of the two constructs; PDB:2R4R and PDB:2R4S) were determined using molecular replacement using the immunoglobulin-domain search models for the Fab.

Several regions of the receptor are either unresolved in the crystal structure or obscured by the Fab fragment. In particular, the C-terminal tail region is missing from the engineered-receptor construct, and the C3 loop is bound to the Fab fragment. However, the binding of the Fab apparently did not affect agonist or antagonist binding, and did not prevent the conformational changes concomitant with receptor activation. The ligand binding site can be identified as an extended flat structure near to the extracellular receptor surface, but the carazolol itself is not resolved and the active site of the receptor is not seen in detail. The Fab itself and the TM helices near to the cytoplasmic surface of the receptor are the best-resolved regions of the structure.

In simultaneous work, Cherezov *et al.* [11] engineered a  $\beta_2$ AR with the same modifications in the N- and C-terminal tails and the same N187E substitution. However, instead of using an Fab fragment to stabilize the receptor, they created a fusion protein by inserting a synthetic gene encoding a slightly modified version of the enzyme T4 lysozyme between Ile233(5.72) and Arg260(6.22). The  $\beta_2$ AR–T4 lysozyme fusion construct was also expressed in *Sf9* insect cells and purified by a method very similar to that of Rasmussen *et al.* Final diffraction data from more than 40 crystals were considered to obtain a full dataset at complete 2.4-Å resolution. Initial phases of the construct were obtained by molecular replacement using both T4 lysozyme and a polyamine model of rhodopsin as search models. Most likely due to the use of the LCP method, the quality of the structure reported by Cherezov *et al.* [11] (PDB:2RH1) is superior to that reported by Rasmussen *et al.* [13].

Excellent quality electron density is observed for residues 29 to 342 of the 365 amino-acid full-length construct. Two disulfide bonds, Cys106–Cys191 and Cys184–Cys190, are observed, and a palmitic acid linked to Cys341 is clearly visible in the  $F_o - F_c$  omit maps. Importantly, the active site contains a well-resolved carazolol ligand. The borders of all of the TM helices and loops can be defined from the structure, except, of course, where the T4 lysozyme was introduced in the C3 loop. Interestingly, a short helical segment near to the middle of the E2 loop is seen, which is not present in rhodopsin and was also not predicted by automated secondary structure prediction algorithms. Interactions between residues of the T4 lysozyme and receptor components are discussed in some detail in Cherezov *et al.* [11]. Basically, there are minimal intermolecular interactions between the T4 lysozyme component of one molecule and the receptor component of a neighboring molecule in the LCP crystal lattice, and it is argued that these interactions cause no particular structural perturbation.

It is informative to compare and contrast the structures of rhodopsin and the  $\beta_2$ AR. The N-terminus of the  $\beta_2$ AR is disordered, whereas that of rhodopsin is resolved clearly and interacts extensively with extracellular domains and forms a small four-strand  $\beta$ -sheet in concert with the E2 loop, which essentially blocks access to the retinal binding site [21]. In the  $\beta_2$ AR a short helical segment on the E2 loop, which includes a disulfide-bonded Cys, sits well above the carazolol binding site. Carazolol and retinal are situated in similar binding sites in the core of the helical bundle, but near to the extracellular surface. The TM helical segments of rhodopsin and  $\beta_2$ AR superimpose nearly precisely, except for TM helix 1. The TM helix 1 of  $\beta_2$ AR, despite containing a Pro not found in rhodopsin, is straight, and angled away from the axis of the receptor by about 18°.

The functional properties of the expressed  $\beta_2$ AR–T4 lysozyme fusion construct were studied in detail [12]. In

p0080

p0050

p0090

p0060

p0100

p0110

p0070

summary, the construct bound the antagonist [<sup>3</sup>H]-dihydroalprenolol (DHA) and the inverse agonist ICI-118,551 with the same affinities as the native expressed receptor. However, the affinities of the engineered construct for agonists (isoproterenol, epinephrine and formoterol) and partial agonist (salbutamol) were two- to three-fold higher than those of the native receptor. A shift in agonist affinity is associated with constitutive receptor activity, and it is possible that the engineered receptor conformation, at least in membranes, is partially active. The engineered receptor fusion could not bind to heterotrimeric G proteins. However, studies of a receptor construct containing a fluorescent probe linked to Cys265 at the cytoplasmic end of TM helix 6 were consistent with a partial active conformational equilibrium. Finally, when compared with the structure of the  $\beta_2$ AR solved in complex with the Fab fragment, one prominent difference is the altered packing of Phe264 at the cytoplasmic end of TM helix 6 in the fusion receptor. In the  $\beta_2$ AR–Fab complex, the interactions between Phe264 and residues in TM helices 5 and 6, and the C2 loop, may be important in maintaining  $\beta_2$ AR in its basal “off” state [12].

How can the  $\beta_2$ AR crystal structure be used to gain a better understanding of ligand–receptor interactions and receptor activation? One approach is to employ advanced computational molecular dynamics (MD) simulations. For example, a recent MD simulation placed the receptor bound to carazolol in a typical bilayer membrane environment, and then addressed the question of whether or not the agonist ligand, adrenaline, would itself be stable in fundamentally the same receptor structural conformation as when it binds carazolol [20]. The nanosecond timescale of these MD simulations was certainly not sufficient to capture the slow transition to the active receptor conformation. However, a principal component analysis of the movements of the backbone C $\alpha$  atoms demonstrated a global change of the receptor structure in its transition from the carazolol- to the adrenaline-bound form. The change is consistent with the elongated structure of the antagonist pushing the extracellular ends of TM helices 2 and 6 outward into the bilayer, and of TM helix 7 toward water. In fluorescently labeled  $\beta_2$ AR (tetramethylrhodamine-5-maleimide labeled at Cys265(6.27), or monobromobimane labeled at Cys271(6.33)) in detergent, noradrenaline induces a change in fluorescence with biphasic kinetics of 2.8-s and 70-s half-life times of the fast and slow phases, respectively [30–32]. However, the activation kinetics in cyan-fluorescent protein/yellow-fluorescent protein (CFP/YFP) fusion constructs of  $\alpha_2$ AR *in vivo* with comparable ligand concentrations is significantly faster. Noradrenaline induces a conformational change within about 40 ms [33], but the time traces appear to contain a second slow phase in the seconds timescale. Possible reasons for this difference in activation rates compared to  $\beta_2$ AR have been discussed; for example, the presence of the cell membrane and G proteins *in vivo* [34].

p0140

## s0040 UNDERSTANDING LIGAND BINDING SPECIFICITY IN GPCRS

p0120 The central dogma in GPCR molecular pharmacology is that receptor activation and desensitization are both mediated via strictly stimulus-dependent interaction of the receptor with another protein (heterotrimeric G protein, G-protein-coupled receptor kinases, and  $\beta$ -arrestins) [22]. The ternary complex of agonist, receptor, and G protein is believed to trigger allosterically nucleotide exchange on the G protein. The consequence is that agonist binding to the receptor should exhibit allosteric modulation by the G protein. In the absence of the G protein, the binding affinity for agonists is typically reduced [23]. The question is whether or not the agonist–receptor complex can formally switch to the active conformation without the G protein. Receptor activation is accompanied by movement of cytoplasmic end of TM helix 6, as demonstrated by restraints imposed by engineered metal ion binding sites [24] and disulfide bridges [25], and by interaction of spin labels on double cysteine mutants [25,26].

s0050

p0150

In rhodopsin, photon capture isomerizes the inverse agonist form of the covalently-bound 11-*cis*-retinylidene ligand to the all-*trans* agonist form. Chromophore isomerization results in large conformational changes, as demonstrated by several biophysical methods [27]. It should be noted that rhodopsin also functions as a receptor for diffusible ligands, such as all-*trans*-retinal [28], even though its standard function is mediated by the covalently-bound ligand, which allows detection of photons. Moreover, in a mutant receptor K296G, an artificial amine ligand binds and activates as a strictly diffusible ligand [29].

## STRUCTURAL BASIS OF THE ACTIVE STATE

Do any of the new crystal structures correspond to that of a constitutively active basal state? A constitutively active receptor is expected to have higher agonist binding affinities in the absence of G proteins. The  $\beta_2$ AR–T4L fusion protein, compared with  $\beta_2$ AR, exhibits higher affinities for agonists, such as (–)-isoproterenol and (–)-epinephrine [12]. The experiments were performed in Sf9 membranes in the absence of GTP. In Sf9 membranes  $\beta_2$ AR does not contain sufficient G-protein concentrations to exhibit a GTP-sensitive high-affinity receptor form [23]. The higher agonist affinity is consistent with constitutive activity of the fusion protein. Moreover, the ligand-dependent changes in fluorescence of bimane-labeled Cys265 indicate an altered basal state [12]. Interestingly, the crystal structure shows that Glu268(6.30) interacts with T4L instead of Arg131(3.50) in the conserved E(D)RY motif at the cytoplasmic end of TM helix 3 [12]. Arg131(3.50) interacts with Asp130(3.29)

p0130

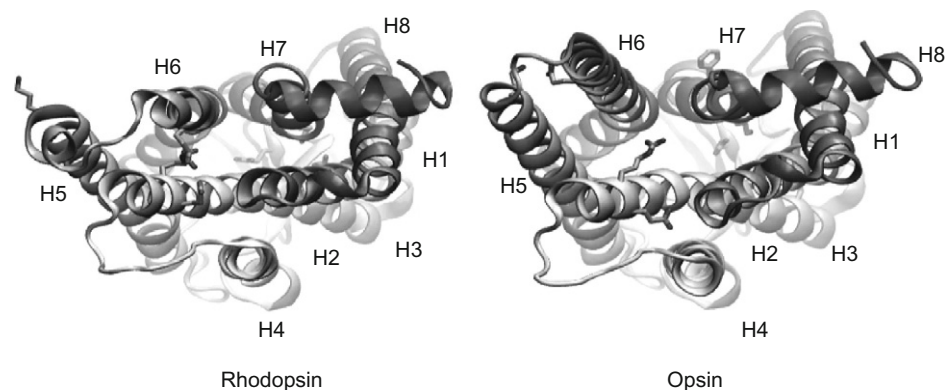


**FIGURE 23.1 Comparison of structures of the structures of rhodopsin and “active” opsin.**

Backbone ribbon depictions are presented for rhodopsin (PDB:1GZM) (left) and opsin (PDB:3CAP) (right). The view is from the cytoplasmic surface side of the receptor. Helices are progressively shaded from light gray (H1) to dark gray (cytoplasmic amphipathic helix 8). The 11-*cis*-retinylidene chromophore is removed from the rhodopsin structure for clarity. Several key structural changes are noted. The cytoplasmic surface is generally more opened in the opsin structure. H6 moves outward and rotates, affecting the orientation of “ionic lock” residues. The distance between Lys296 on H7 and Glu113 on H3 increases, and the distance between Lys296 and Glu181 on the E3 loop decreases. The structure of the E3 loop changes dramatically and small pores appear between H5 and H6 and H7 and H1 (these changes are not well seen in this depiction, however).

f0010  
AUQ1

and a sulfate ion, and in the MD simulations there is evidence for local density of chloride ions. It has been shown that the E268A(6.30) substitution in a  $\beta_2$ AR-G $\alpha_s$  fusion protein results in higher agonist affinity for the low affinity state [35]. Based on homology with rhodopsin, the “ionic lock” formed by Asp130(3.49), Arg131(3.50), and Glu268(6.30) is thought to stabilize the inactive receptor conformation. Both Shukla *et al.* [36] and Rosenbaum *et al.* [12] concluded that their crystal structures may in fact represent an “active-like state” or a “partial constitutively active” receptor, respectively.

p0160

The structure of ligand-free opsin, however, most certainly represents an active-state structure (Figure 23.1). Compared with rhodopsin, prominent structural changes are noted in the highly conserved E(D)RY and NpXXY(x)5,6F regions, and in H5–H7. Furthermore, H6 is tilted out by a remarkable 6–7 $\text{\AA}$ . A follow-up study reported the structure of the complex of opsin with an 11-amino acid residue peptide from the alpha-subunit of the rod cell G protein, transducin. This peptide was known to bind to light-activated rhodopsin and to stabilize the active state of rhodopsin called metarhodopsin II. The bound peptide makes extensive contacts with opsin along the inner surface of H5 and H6, which induce a helical structure in the peptide not found in solution. If confirmed to be the active-state structure, the “helix movement model” of receptor activation would be validated. The challenge now remains to obtain the structure of the complex between an agonist-bound GPCR and a G protein.

## REFERENCES

- Overington JP, Al-Lazikani B, Hopkins AL. How many drug targets are there? *Nature Rev Drug Discov* 2006;**5**:993–6.
- Han M, Smith SO, Sakmar TP. Constitutive activation of opsin by mutation of methionine 257 on transmembrane helix 6. *Biochemistry* 1998;**37**:8253–61.
- Robinson PR, Cohen GB, Zhukovsky EA, Oprian DD. Constitutively active mutants of rhodopsin. *Neuron* 1992;**9**:719–25.
- Kjelsberg MA, Cotecchia S, Ostrowski J, Caron MG, Lefkowitz RJ. Constitutive activation of the  $\alpha_1$ B-adrenergic receptor by all amino acid substitutions at a single site. Evidence for a region which constrains receptor activation. *J Biol Chem* 1992;**267**:1430–3.
- Cotecchia S. Constitutive activity and inverse agonism at the  $\alpha_1$  adrenoreceptors. *Biochem Pharmacol* 2007;**73**:1076–83.
- Parnot C, Miserey-Lenkei S, Bardin S, Corvol P, Clauser E. Lessons from constitutively active mutants of G protein-coupled receptors. *Trends Endocrinol Metab* 2002;**13**:336–43.
- Palczewski K, Kumasaka T, Hori T, Behnke CA, Motoshima H, Fox BA, Le Trong I, Teller DC, Okada T, Stenkamp RE, Yamamoto M, Miyano M. Crystal structure of rhodopsin: A G protein-coupled receptor. *Science* 2000;**289**:739–45.
- Nakamichi H, Okada T. Crystallographic analysis of primary visual photochemistry. *Angew Chem Intl Ed Engl* 2006;**45**:4270–3.
- Nakamichi H, Okada T. Local peptide movement in the photoreaction intermediate of rhodopsin. *Proc Natl Acad Sci USA* 2006;**103**:12729–34.
- Nakamichi H, Buss V, Okada T. Photoisomerization mechanism of rhodopsin and 9-*cis*-rhodopsin revealed by x-ray crystallography. *Biophys J* 2007;**92**:L106–8.
- Cherezov V, Rosenbaum DM, Hanson MA, Rasmussen SG, Thian FS, Kobilka TS, Choi HJ, Kuhn P, Weis WI, Kobilka BK, Stevens RC. High-resolution crystal structure of an engineered human  $\beta_2$ -adrenergic G protein-coupled receptor. *Science* 2007;**318**:1258–65.
- Rosenbaum DM, Cherezov V, Hanson MA, Rasmussen SG, Thian FS, Kobilka TS, Choi HJ, Yao XJ, Weis WI, Stevens RC, Kobilka BK. GPCR engineering yields high-resolution structural insights into  $\beta_2$ -adrenergic receptor function. *Science* 2007;**318**:1266–73.
- Rasmussen SG, Choi HJ, Rosenbaum DM, Kobilka TS, Thian FS, Edwards PC, Burghammer M, Ratnala VR, Sanishvili R, Fischetti RF, Schertler GF, Weis WI, Kobilka BK. Crystal structure of the human  $\beta_2$  adrenergic G-protein-coupled receptor. *Nature* 2007;**450**:383–7.

14. Warne A, Serrano-Vega MJ, Baker JG, Moukhametzianov R, Edwards PC, Henderson R, Leslie AGW, Tate CG, Schertler GFX. Structure of the  $\beta$ 1-adrenergic G protein-coupled receptor. *Nature* 2008;**454**:486–92.
15. Jaakola VP, Griffith MT, Hanson MA, Cherezov V, Chien EY, Lane JR, Ijzerman AP, Stevens RC. The 2.6-Ångstrom crystal structure of a human A2A adenosine receptor bound to an antagonist. *Science* 2008;**Oct 2** [Epub ahead of print].
16. Murakami M, Kouyama T. Crystal structure of squid rhodopsin. *Nature* 2008;**453**:363–7.
17. Shimamura T, Hiraki K, Takahashi N, Hori T, Ago H, Masuda K, Takio K, Ishiguro M, Miyano M. Crystal structure of squid rhodopsin with intracellularly extended cytoplasmic region. *J Biol Chem* 2008;**283**:17753–6.
18. Park JH, Scheerer P, Hofmann KP, Choe H-W, Ernst OP. Crystal structure of the ligand-free G-protein-coupled receptor opsin. *Nature* 2008;**454**:183–7.
19. Scheerer P, Park JH, Hildebrand PW, Kim YJ, Krauss N, Choe H-W, Hofmann KP, Ernst OP. Crystal structure of opsin in its G-protein-interacting conformation. *Nature* 2008;**455**:497–503.
20. Huber T, Menon S, Sakmar TP. Structural basis for ligand binding and specificity in adrenergic receptors: Implications for GPCR-targeted drug discovery. *Biochemistry* 2008. in press.
21. Menon ST, Han M, Sakmar TP. Rhodopsin: structural basis of molecular physiology. *Physiol Rev* 2001;**81**:1659–88.
22. Lefkowitz RJ. Seven transmembrane receptors: something old, something new. *Acta Physiol (Oxf)* 2007;**190**:9–19.
23. Seifert R, Lee TW, Lam VT, Kobilka BK. Reconstitution of  $\beta$ 2-adrenoceptor-GTP binding-protein interaction in Sf9 cells – high coupling efficiency in a  $\beta$ 2-adrenoceptor-Gs $\alpha$  fusion protein. *Eur J Biochem* 1998;**255**:369–82.
24. Sheikh SP, Zvyaga TA, Lichtarge O, Sakmar TP, Bourne HR. Rhodopsin activation blocked by metal-ion binding sites linking transmembrane helices C and F. *Nature* 1996;**383**:347–50.
25. Farrens DL, Altenbach C, Yang K, Hubbell WL, Khorana HG. Requirement of rigid-body motion of transmembrane helices for light activation of rhodopsin. *Science* 1996;**274**:768–70.
26. Altenbach C, Kusnetzow AK, Ernst O, Hofmann KP, Hubbell WL. High resolution distance mapping in rhodopsin reveals the pattern of helix movement due to activation. *Proc Natl Acad Sci USA* 2008;**105**:7439–44.
27. Shieh T, Han M, Sakmar TP, Smith SO. The steric trigger in rhodopsin activation. *J Mol Biol* 1997;**269**:373–84.
28. Cohen GB, Oprian DD, Robinson PR. Mechanism of activation and inactivation of opsin – role of Glu113 and Lys296. *Biochemistry* 1992;**31**:12592–601.
29. Zhukovsky EA, Robinson PR, Oprian DD. Transducin activation by rhodopsin without a covalent bond to the 11-cis-retinal chromophore. *Science* 1991;**251**:558–60.
30. Swaminath G, Xiang Y, Lee TW, Steenhuis J, Parnot C, Kobilka BK. Sequential binding of agonists to the  $\beta$ 2 adrenoceptor. Kinetic evidence for intermediate conformational states. *J Biol Chem* 2004;**279**:686–91.
31. Swaminath G, Deupi X, Lee TW, Zhu W, Thian FS, Kobilka TS, Kobilka B. Probing the  $\beta$ 2 adrenoceptor binding site with catechol agonists. *J Biol Chem* 2005;**280**:22165–71.
32. Yao X, Parnot C, Deupi X, Ratnala VR, Swaminath G, Farrens D, Kobilka B. Coupling ligand structure to specific conformational switches in the  $\beta$ 2-adrenoceptor. *Nat Chem Biol* 2006;**2**:417–22.
33. Vilardaga JP, Bunemann M, Krasel C, Castro M, Lohse MJ. Measurement of the millisecond activation switch of G-protein-coupled receptors in living cells. *Nature Biotechnol* 2003;**21**:807–12.
34. Lohse MJ, Hoffmann C, Nikolaev VO, Vilardaga JP, Bunemann M. Kinetic analysis of G-protein-coupled receptor signaling using fluorescence resonance energy transfer in living cells. *Adv Protein Chem* 2007;**74**:167–88.
35. Ghanouni P, Schambye H, Seifert R, Lee TW, Rasmussen SG, Gether U, Kobilka BK. The effect of pH on  $\beta$ 2 adrenoceptor function. Evidence for protonation-dependent activation. *J Biol Chem* 2000;**275**:3121–7.
36. Shukla AK, Sun JP, Lefkowitz RJ. Crystallizing thinking about the  $\beta$ 2-adrenergic receptor. *Mol Pharmacol* 2008;**73**:1333–8.
37. Teller DC, Okada T, Behnke CA, Palczewski K, Stenkamp RE. Advances in determination of a high-resolution three-dimensional structure of rhodopsin, a model of G-protein-coupled-receptors (GPCRs). *Biochemistry* 2001;**40**:7761–72.
38. Okada T, Fujiohshi Y, Silow M, Navarro J, Landau EM, Schichida Y. Functional role of internal water molecules in rhodopsin revealed by X-ray crystallography. *Proc Natl Acad Sci USA* 2002;**99**:5982–7.
39. Okada T, Sugihara M, Bondar AN, Elstner M, Entel P, Buss V. The retinal conformation and its environment in rhodopsin in light of a new 2.2-Å crystal structure. *J Mol Biol* 2004;**342**:571–83.
40. Li J, Edwards PC, Burghammer M, Villa C, Schertler GF. Structure of bovine rhodopsin in a trigonal crystal form. *J Mol Biol* 2004;**343**:1409–38.
41. Salom D, Lodowski DT, Stenkamp RE, Trong IL, Golczak M, Jastrzebska B, Harris T, Ballesteros JA, Palczewski K. Crystal structure of a photoactivated deprotonated intermediate of rhodopsin. *Proc Natl Acad Sci USA* 2006;**103**:16123–8.
42. Standfuss J, Xie G, Edwards PC, Burghammer M, Oprian DD, Schertler GF. Crystal structure of a thermally stable rhodopsin mutant. *J Mol Biol* 2007;**372**:1179–88.
43. Hanson MA, Cherezov V, Griffith MT, Roth CB, Jaakola VP, Chien EY, Velasquez J, Kuhn P, Stevens RC. A specific cholesterol binding site is established by the 2.8 Å structure of the human  $\beta$ 2-adrenergic receptor. *Structure* 2008;**16**:897–905.

#### Author Query

{AUQ1} Please provide high resolution figure.